

Ali ALAVI NIA,<sup>1</sup> Saeed AMIRCHAKHMAGHI<sup>2</sup>

## Investigating the effects of alumina nanoparticles on the impact resistance of polycarbonate nano-composites

Received 28 August, 2021, Revised 24 January 2022, Accepted 16 February 2022, Published online 6 May 2022

**Keywords:** nanoparticles, alumina, ballistic test, nano-composite, polycarbonates, surface treatments

In this project, two types of treated and untreated alumina nanoparticles with different weight percentages (wt%) of 0.5, 1 and 3% were mixed with polycarbonate matrix; then, the impact ballistic properties of the nano-composite targets made from them were investigated. Three types of projectile noses -cylindrical, hemispherical, and conical, each with the same mass of 5.88 gr – were used in the ballistic tests. The results highlighted that ballistic limit velocities were improved by increasing the percentage of alumina nanoparticles and the treatment process; changing the projectile's nose geometry from conical to blunt nose increases the ballistic limit velocity, and ultimately, by increasing the initial velocity of conical and hemispherical nosed projectiles, the failure mechanism of the targets changed from dishing to petalling; whereas for the cylindrical projectile, the failure mode was always plugging.

### 1. Introduction

Polycarbonate is one of the engineering polymers which has always been taken into consideration in various industries, owing to its specific properties, especially automotive and aerospace [1]. Because of its high impact resistance, this material has been used in helmets, bulletproof vests and vehicle productions [2, 3]. Also, where a transparent material with good impact resistance is needed, polycarbonate is usually one of the top choices. For instance, polycarbonate has been used as a material for preparing riot shields [4]. Thanks to these properties, the usage of this

✉ Saeed AMIRCHAKHMAGHI, e-mail: [e.s.amirchakhmaghi@gmail.com](mailto:e.s.amirchakhmaghi@gmail.com)

<sup>1</sup>Department of Mechanical Engineering, Bu Ali Sina University, Hamedan, Iran

<sup>2</sup>Department of Mechanical Industrial and Aerospace engineering, Concordia University, Montreal, Canada



© 2022. The Author(s). This is an open-access article distributed under the terms of the Creative Commons Attribution-NonCommercial-NoDerivatives License (CC BY-NC-ND 4.0, <https://creativecommons.org/licenses/by-nc-nd/4.0/>), which permits use, distribution, and reproduction in any medium, provided that the Article is properly cited, the use is non-commercial, and no modifications or adaptations are made.

polymer, or composites made from this polymer matrix, has been a common place in the production of components such as windscreens and headlights, as well as polymeric windows instead of common windows in buildings [5].

Because of the many applications of polycarbonate in the different industries – namely safety productions – investigating its impact resistance and ballistic properties has always been a popular research topic with scientists. As a case in point, Wright et al. [6] studied the ballistic properties of polycarbonate in a project in 1992. They prepared some plates from the polycarbonate, and shot flat and hemispherical projectiles at them. Then, they reported that the ballistic limit velocity and phenomena such as penetration, perforation, dishing, and petalling had occurred in the plates. In another study, ballistic properties of riot shields made from polycarbonate in various conditions were investigated by Edwards and Waterfall, using different projectiles – mainly ball bearing, golf ball and brick [4]. The effect of distance from the support on the penetration mechanism of clamped polycarbonate plates was investigated by Shah and Abkar [2]. They fixed circular polycarbonate plates with a diameter of 115 mm and a thickness of 1.91 mm by a fixture. After that, they shot the spherical projectiles with the same diameter of 6.98 mm and the constant velocity of 138 m/s at the fixed plates in the distances of 0, 10, 20, 30, 40 and 50 mm from the central point of the plates. They then reported the results such as penetration depth and plate thickness after different shooting conditions.

Given the mentioned cases, the importance of ballistic impact resistance of the polycarbonate plates is increasingly growing. Therefore, new methods of improving their impact resistance have constantly been investigated. One such method is composing nano-composites which contain nano-size fibers and particles inside polymer matrix. Rahman et al. [7] studied the effect of adding amino-functionalized multi-walled carbon nanotubes (NH<sub>2</sub>-MWCNTs) on the ballistic performance of E-glass/epoxy composites. They used a gas gun for investigating the ballistic performance of the composite and learned that the ballistic limit velocity of this composite had increased virtually by 5 percent. Kalkurni et al. [8] investigated ballistic and blast performance of current and future candidate materials for helmets such as nano-composites and thermoplastic polymers. Also, they discussed the mechanisms of ballistic energy absorption, effects of helmet curvatures on ballistic performance, and performance measures of helmets. On the other study, the effect of carbon nanotubes (CNT) on the mechanical response of polycarbonate to dynamic load and high velocity impacts investigated by Al-Lafi et al. [9]. They observed a dramatic increase in the impact resistance, impact failure energy and fracture toughness of the polycarbonate nano-composites.

Given the special properties of alumina particles, such as abrasion resistance, hardness and corrosion resistance in high temperatures, they have always been used as proper fillers for improving the thermal, mechanical and electrical properties of different materials. Owing to the lightness and high ratio of strength to mass, producing metal matrix composites based on aluminum ma-

trix containing alumina particles has been a common trend in the automotive and aerospace industries. Special properties of alumina particles give them an optimized combination of both high ductility and high strength in the composite Al-Al<sub>2</sub>O<sub>3</sub>. In this regard, Kurzawa et al. [10] obtained impressive results from their investigation into the Al-Al<sub>2</sub>O<sub>3</sub> composite. They studied the ballistic impact resistance of aluminum casting alloy 7075 reinforced by Al<sub>2</sub>O<sub>3</sub> particles, numerically and experimentally. The results indicated that alumina particles improved the impact resistance of aluminum matrix. Moreover, these special properties of alumina particles has turned them into vastly applicable materials in nano-composites [11]. Owing to their dielectric properties, polymer nano-composites containing alumina nanoparticles have been used in miniaturized electrical devices. Jacob et al. [12] investigated the mechanism of dielectric enhancement in polymer-alumina nano-composites by studying the molecular interactions between an alumina nanoparticle surface and a polymer matrix. On the other hand, it has been indicated that by adding these nanoparticles to the polycarbonate matrix, the failure strain and energy absorption increase in the composed nano-composite. Given the previously-mentioned properties of alumina nanoparticles, they can be a good option as fillers in the preparation of a nano-composite, based on polycarbonate matrix, to improve its ballistic impact resistance.

Treating alumina nanoparticles and preparing them before adding them to the polymer matrix gives them a better distribution in their matrix [13]. To investigate the properties of a nano-composite epoxy-alumina, Zhao et al. [14] have treated the alumina nanoparticles in a process by using a coupling agent silane named 3-Aminopropyltriethoxysilane (APTES). But, this process is extremely complex and takes a long time. Hence, in the process of their nano-composites combination (epoxy-alumina), Zunjarrao et al. [15] added the coupling agent directly to the polymer matrix, during the mixing time of the nano-fillers with the matrix, in a simple way by using ultrasonic equipment in an hour. Also, in another project, the mechanical properties of nano-composite with polycarbonate matrix as well as alumina nanoparticles were obtained [16].

As it was discussed earlier, the ballistic properties of polycarbonate plates in front of different projectile impacts have already been investigated. But the effect of nano-alumina fillers and their treatment process on the impact resistance of this polymer matrix is yet to be determined. The purpose of this article is to empirically find a way to increase the ballistic impact resistance of a polycarbonate matrix. Relying on the previous literatures referred earlier, adding the certain amount of alumina nanoparticles helps one to reach the goal. Hence, taking the previous work into account [16], three weight percentages of 0.5, 1 and 3% of alumina nanoparticles were mixed at the polycarbonate matrix by using an extruder. Also, some nano-composites containing alumina nanoparticles, which had been treated by coupling agent silane APTES, were prepared as well. After producing nano-composite granules, the nano-composite plates for ballistic tests were molded using

an injection molding process [16]. Then, three types of projectiles, cylindrical, hemispherical and conical with the same mass of 5.8 g, were prepared and shot at the nano-composite targets. Finally, the impact resistance of nano-composites, such as ballistic limit velocity, was determined by shooting 130 different types of projectiles at the nano-composite plates. In order to fully test and determine the ballistic limit velocity and failure mechanism of the targets, the effects of the following factors were carefully monitored: adjusting the proportion of nano-contents, enhancing the velocity of the projectiles, changing the nose geometry of the projectiles, and noting the treatment process of alumina nanoparticles. Also, it is tried to find the plausible reasons for the results obtained from the tests.

## 2. Ballistic limit velocity

Ballistic limit velocity ( $v_{50}$ ) could be defined as the least velocity of projectile for completing penetration and passing through the target thickness [17]. Ballistic limit velocity could be calculated by finding the relationship between the incident and residual velocities of the projectile by using an appropriate curve fitting and finding the point where the residual velocity equals zero ( $v_r = 0$ ). Diverse methods are available for curve fitting; however, Eq. (1), called Jonas-Lambert, which has been used in many papers [17], is applied to the collected experimental data. Ballistic limit velocity is obtained by determining the coefficients of this equation and its root.

$$v_r^P = A (v_i^P - v_{50}^P) = Av_i^P - B. \quad (1)$$

In this equation,  $v_i$  and  $v_r$  represent the projectile velocity before the impact or the incident velocity, and projectile velocity after the impact or the residual velocity, respectively. Also,  $A$  and  $B$  represent the constant coefficients, and  $P$  represents a constant number. This equation is derived from the law of conservation of energy as it is shown in Eq. (2) [17].

$$\frac{1}{2}m_i v_i^2 = \frac{1}{2}m_i v_r^2 + E, \quad (2)$$

where the left side of the equation is the kinetic energy of the projectile before incident and the right side of the equation consists of kinetic energy of the projectile after incident plus the term  $E$ . It can be described as the energy consumed when limit velocity occurs (3).

$$E = \frac{1}{2}m_l v_{50}^2. \quad (3)$$

Substituting Eq. (3) in (2) with an assumption that the projectile has the same mass before and after the incident, Eq. (4) is obtained:

$$v_r^2 = v_i^2 - v_{50}^2. \quad (4)$$

So, if the power 2 changes to  $P$  and we add an  $A$  term, any errors owing to some assumptions (ex. mass elimination) can be described by fitting different powers to experimental data [17]. It should not be left unmentioned that Jonas-Lambert equation is identified as the Recht-Ipson equation if the term  $P$  swaps to 2.

### 3. Experiments

#### 3.1. Materials

The alumina nanoparticles ( $\gamma$  phase and Specific Surface Area (SSA) = 160 m<sup>2</sup>/g) used in this project, with an average particle size of 20 nm, were purchased from an American company. The coupling agent APTES (material code: 821619; SSA = 353 m<sup>2</sup>/g) used in this work was supplied by the German company of Merck. Also, the polycarbonate used as a polymer matrix was Marklon 2870 from German Bayer Company with a density of 1200 kg/m<sup>3</sup> and  $T_g$  of 144°C, whose properties are shown in Table 1 [18].

Table 1. Properties of materials

Standard	Value	Properties
ISO 527-1,-2	2400 MPa	Elasticity module
ISO 527-1,-2	66 MPa	Yield stress
ISO 527-1,-2	130%	Strain at break
ISO179-1eA	75 (kJ/m <sup>2</sup> ) (partial break at 23°)	Charpy notched impact
ISO 11357-1,-2	144°	Glass transition temperature

#### 3.2. The process of nano-composites preparation

Using coupling agent silane, the alumina nanoparticles treatment process was performed according to Chandra's studies [19] in the chemistry laboratory of Bu-Ali Sina University. Step by step of this process was reported in our previous work [16]. Also, nano-composites with specimens' codes and weight percentage of nano size contents written in Table 2 were co-extruded by using the DSE25 twin screw

Table 2. Specimens' codes used in nano-composites combination related to the wt% of nano contents

	Specimens' codes						
	Pc-neat	Al-No-T-0.5	Al-No-T-1	Al-No-T-3	Al-T-0.5	Al-T-1	Al-T-3
Fillers	–	Untreated alumina	Untreated alumina	Untreated alumina	Treated alumina	Treated alumina	Treated alumina
Wight percentage of fillers	–	0.5%wt	1%wt	3%wt	0.5%wt	1%wt	3%wt

extruder (Brabender – Germany) and the master batch method. Then, an injection molding machine (supplied by Iraj Co., Iran) was used to prepare the square plates ( $100 \times 100 \text{ mm}^2$ ) with the thickness of 4 mm. It should be mentioned that the specimens' codes in Table 2 are valid until the end of the paper by considering the wt% of nanoparticles and their treatment process.

### 3.3. Ballistic tests

In order to find the ballistic limit velocity, the projectile velocity needed to be determined before and after hitting. Afterwards, the ballistic limit velocity could be obtained by plotting the  $v_i - v_r$  diagram and finding the coefficients of Jonas-Lambert equation and its root. Thereafter, 130 specimens of nano-composites containing different weight percentages of alumina nanoparticles were prepared (as in Table 2) for the ballistic tests.

Gas gun equipment (available at the laboratory of mechanical behavior of materials, Bu-Ali Sina University) was used to shoot the projectiles at the targets. As it is depicted in Fig. 1, this gas gun was comprised of two main parts, the pressure vessel and the barrel. The consuming gas entered the vessel and was compressed up to a certain pressure point. Afterward, by opening the shooting valve and under a mechanism, this compressed gas left the pressure behind the projectile and caused movement in the gun's barrel. Obviously, increasing the pressure level enhanced the projectile's velocity. Certainly, due to the acceleration of the gas's mass alongside the projectile's mass at the high pressure levels, the output velocity of the projectile from the barrel's gun did not alter as the pressure level increased. It should be asserted that achieving a higher hitting velocity in certain gas pressure points and the projectile mass could be feasible as long as a lighter-mass gas was used in the gas gun.



Fig. 1. Gas gun used for performing ballistic tests

A fixture was designed and constructed in order to fix the targets perpendicularly in front of the gun's barrel. In this case, the square target plates ( $100 \times 100 \text{ mm}^2$ )

were uniformly kept in front of the gun's barrel by the help of a hollow plate (Fig. 2) and 18 screws (M6) up to 15 mm from each side of them. There remained a square hole – with the area of  $70 \times 70 \text{ mm}^2$  – which was filled by the target plate thickness. In this condition, different failure mechanisms were experienced in the targets by passing the 11 caliber projectiles from them, without the effects of boundary conditions.

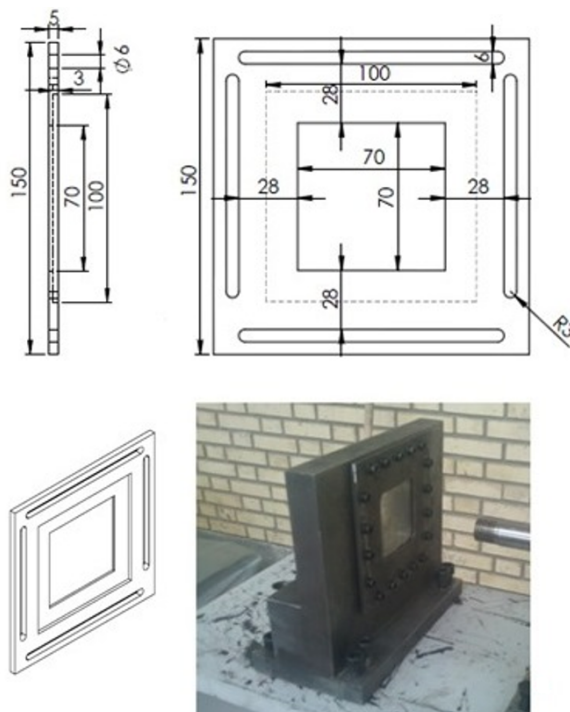


Fig. 2. The illustration of fixture and its draft

Also, two chronographs (supplied by Shooting ChornyM108, USA) were used to determine the projectile's velocities before and after the hitting process. They were able to measure the range of velocities up to 2200 m/s that were indicated on their monitors. The rigid projectiles used in this work were prepared from aluminum 7075-T6, with the diameter of 11 mm, and shaped in three different types of noses – cylindrical, hemispherical and conical, according to Fig. 3. The dimensions of these projectiles were designed in the way that they had similar mass quantities, equaling 5.8 g. The mass was speculated this way in proportion with the projectiles' diameter, so that their buckling and their stepping out of rigidity were prevented.

Each type of projectile, with specific nose geometry, was shot 6 times with the approximate velocities of 80 m/s to 380 m/s at the specimens with the particular material code in order to discover the ballistic limit velocity of nano-composites.

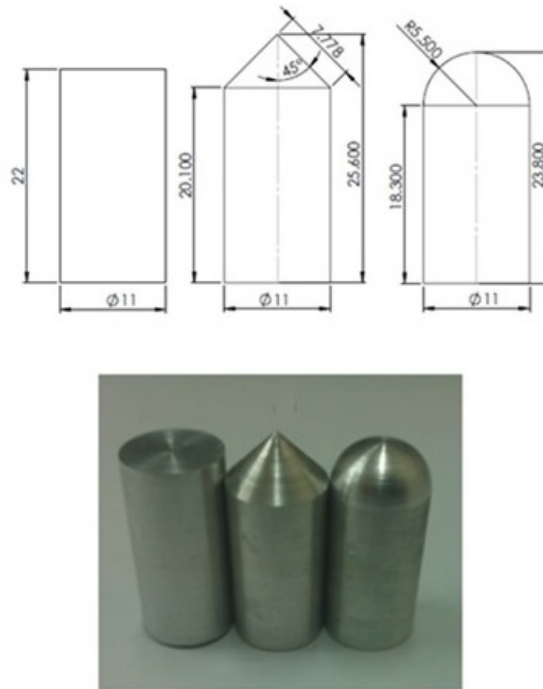


Fig. 3. Projectiles (the dimensions are in millimeter) and projectiles' plan

Thus, for each specimen, 6 shots were performed with specific projectile's nose geometry between seven target material codes, containing different weight percentages of nano-fillers. Better put, 18 shots were performed at one particular material target code containing defined weight percentages of alumina nano-composites. Overall, 126 shots were needed to find the ballistic limit velocities of the nano-composites. Given the error possibilities, 130 shots were performed. An illustration of a target specimen, before and after hitting a projectile, has been illustrated in Fig. 4.



Fig. 4. An illustration of a target before and after hitting a projectile

In some cases, the projectiles were not able to pass through the target since the incident velocities ( $v_i$ ) were too low. In these cases, the projectile just broke the targets (Fig. 5). In other words, the incident velocities were under the ballistic limit velocity, and were not proper to be used in the calculation progress.



Fig. 5. The broken neat polycarbonate target after the hemispherical projectile impact with an incident velocity under the ballistic limit velocity

#### 4. Ballistic limit velocity determination

As it was already mentioned, the incident and residual velocities of each specimen were recorded after shooting each projectile. In order to investigate the effects of changing the failure mechanism, these variables were studied: nose shape of the projectiles as well as the weight percentage of untreated and treated alumina nanoparticles. After recording the incident and the residual velocities, this data was imported into the Matlab software as two matrices for each specimen separately. Then, the Jonas-Lambert equation was applied to the experimental data for different equation powers of  $P = 1.75$ ,  $P = 2$ ,  $P = 2.25$  and  $P = 2.5$ . Its coefficients ( $A$  and  $B$ ) were found by using a special Matlab toolbox named the “curve fitting toolbox”. After that, every obtained equation for the specific projectile nose’s geometry and also different equation powers ( $P$ ) were plotted in a diagram, as illustrated in Figs. 6, 7, and 8. As it was stated above, the points with incident velocities under the ballistic limit velocity were excluded from the calculation process.

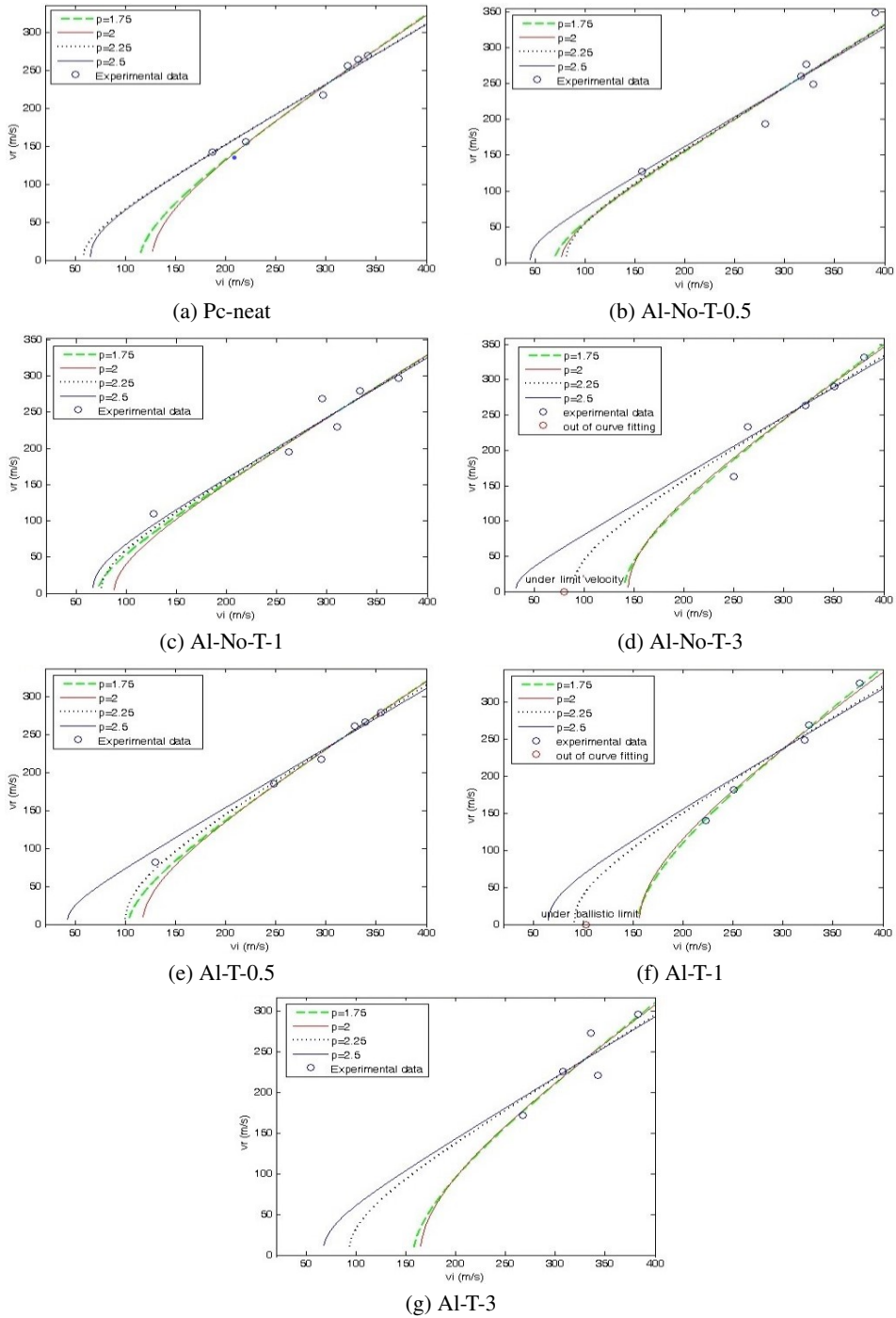


Fig. 6. The ballistic limit diagrams based on Jonas-Lambert equation for different equation powers ( $P$ ) and cylindrical projectiles

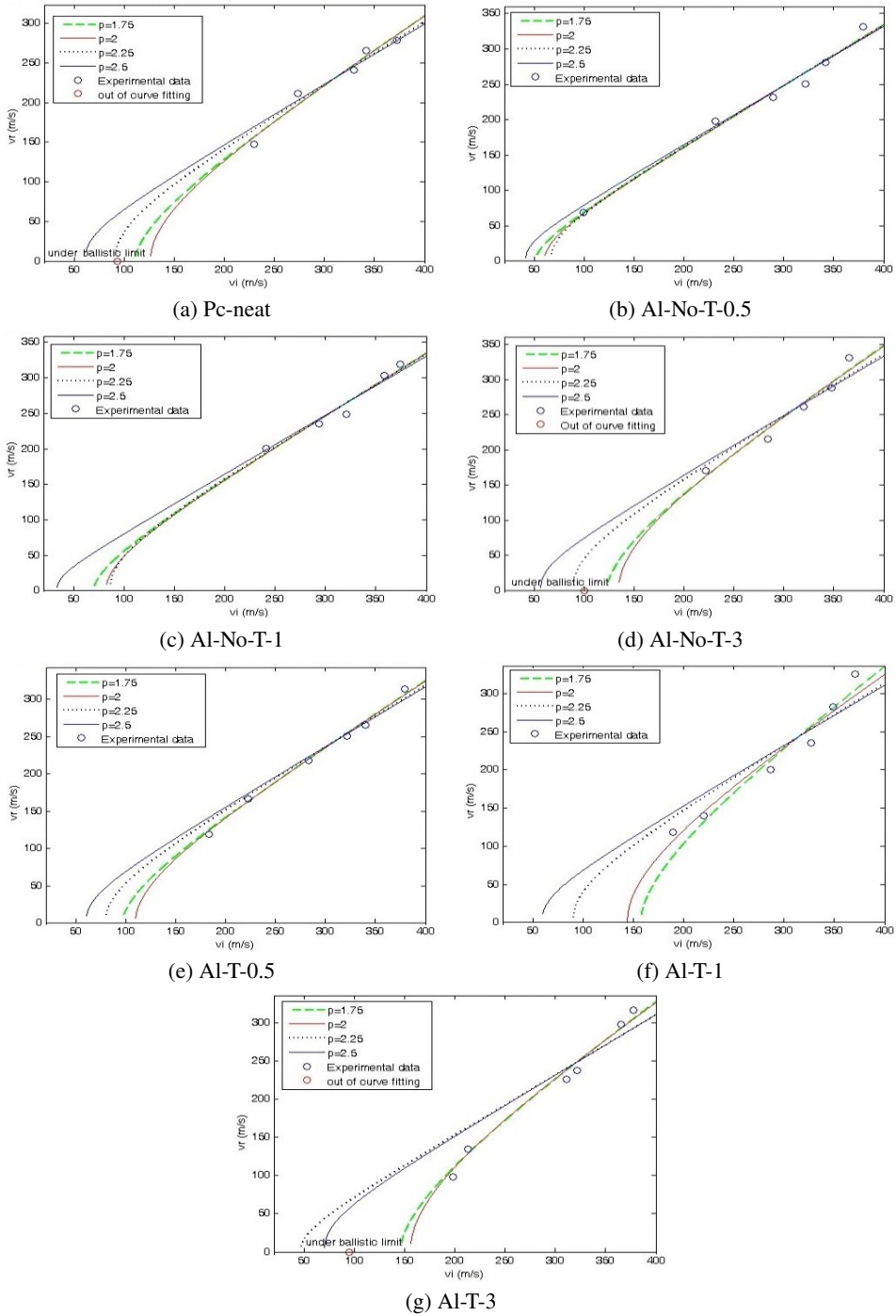


Fig. 7. The ballistic limit diagrams based on Jonas-Lambert equation for different equation powers ( $P$ ) and hemispherical projectiles

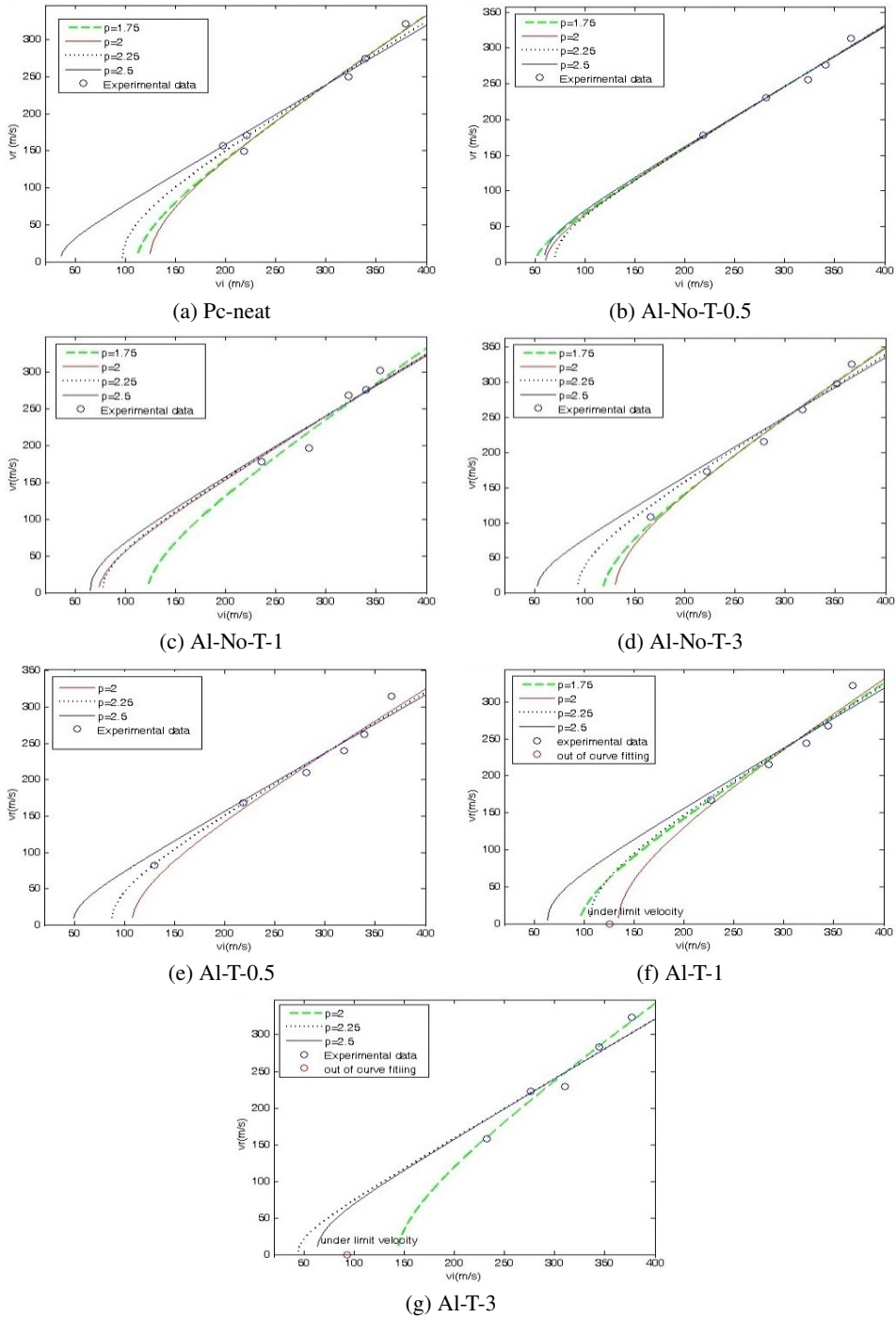


Fig. 8. The ballistic limit diagrams based on Jonas-Lambert equation for different equation powers ( $P$ ) and conical projectiles

## 5. Results and discussion

### 5.1. Ballistic limit velocity

As discussed previously, so as to find the ballistic limit velocities of specimens, the Jonas-Lambert equation was applied to the experimental data points on the  $v_i - v_r$  diagram with different powers ( $P$ ). Based on this, different diagrams from the different equation powers and various specimens were plotted, and illustrated in the previous part. Accordingly, the best plot in every diagram, and obviously its relative ballistic limit velocity, was obtained. On the basis of the theory of Jonas-Lambert equation, in the case its power was assumed to be 2, the Recht-Ipson equation would be obtained. In other words, in the process of proving the equation, initially the power was 2, which had been assumed as an undefined parameter  $P$  to make a safety parameter for possible errors [17, 20]. On the other hand, some points indicated the data with incident velocity under the ballistic limit velocity discussed previously, which was a good guide to exclude the plots assigned to wrong equation power. For instance, in Fig. 8f, the plot assigned power 1.75 must be excluded from the consideration. The reason for this exclusion is because the ballistic limit velocity has to be more than 125.3 m/s, which pointed the case that the projectile had not passed through the target. However, the plot assigned power 1.75 indicates the possible ballistic limit velocity of 95.64 m/s wrongly. Taking all these reasons into consideration and according to the Sum of Squared Errors (SSE) criteria [21], the best match plot for the experimental points was found (Table 3).

Table 3. SSE criteria for finding the best match plot

Projectile shape	$P$	Specimens						
		Pc-neat	Al-No-T-0.5	Al-No-T-1	Al-No-T-3	Al-T-0.5	Al-T-1	Al-T-3
Cylindrical	1.75	147.01	2525.78	1684.93	1547.45	109.28	195.86	1822.84
	2	141.9	2564.96	1688.77	1534.61	107.47	not converged	not converged
	2.25	not converged	2597.49	not converged				
	2.5	not converged						
Hemi-spherical	1.75	429.63	674.86	418.03	769.04	128.98	1790.35	482.76
	2	418.01	671.45	422.41	739.58	122.34	1126.72	448.44
	2.25	not converged	667.45	not converged	not converged	221.20	not converged	not converged
	2.5	not converged	not converged	not converged	not converged	297.14	not converged	not converged
Conical	1.75	not converged	278.33	not converged	353.49	–	775.32	–
	2	338.4	276.54	1207.02	333.60	771.29	769.13	550.01
	2.25	–	not converged	1250.32	not converged	not converged	not converged	not converged
	2.5	not converged	not converged	1353.61	not converged	not converged	not converged	not converged

Considering Table 3, the power  $P$  assigned to the plot with the minimum SSE was chosen as a basic plot in order to find the Jonas-Lambert coefficients ( $A$  and  $B$ ), and finally the ballistic limit velocities. The quantities have been indicated in Table 4. As outlined in this table, ballistic limit velocities increased, as predicted, by blunting the projectile's nose geometry from conical to cylindrical. The nose's shape had an important effect on the target failure. In the hitting process, in front of flexible projectiles with low incident velocities in which the projectile's material is not yielded, blunting the projectile's nose geometry (wider nose) caused an increase in the ballistic limit velocity. Better put, it made the projectile's movement slower in the target's material; whereas at the very high impact velocities, the nose shape did not have a visible effect on the ballistic limit velocity, due to its high erosion in the penetration progress. On the other hand, in the hitting process in front of rigid projectiles, owing to not yielding the projectiles' material, the projectiles with the blunter nose came out from the same targets with the lower velocities; in other words, the ballistic limit velocity increased. This matter was observed in the experimental tests. The projectiles' shape did not change after several shootings, and they were consistently rigid.

The percentage decrease in ballistic limit velocity for different specimens obtained from the hemispherical and conical projectiles hitting in comparison to those obtained from cylindrical projectiles hitting has been shown in Table 5. As illustrated in Table 5, the ballistic limit velocity of specimen Al-No-T-1 (nano-composites containing 1 percent untreated alumina nanoparticles) which was obtained from the cylindrical and also hemispherical projectiles hitting, was lower than the velocity obtained from the conical projectiles. It can be explained by the errors which occurred during the experimental tests, especially in the little amount of data obtained from chronographs.

Each solid filler particle in a polymeric matrix acts as a stress concentration source. An increased force at these points leads to debonding the reaction between the particles and polymer matrix and forms very small local cracks. It means that the matrix can absorb more energy than the pure matrix without the fillers [14, 16]. Linkage of local cracks increases the total crack length and therefore, enhances the ductility impact resistance. More nanoparticles cause more energy absorption for the debonding process and linkage of local cracks. Fig. 9 shows the increase in energy absorption of the nano-composites with increasing the weight percentage of nano-fillers [16]. Other mechanical properties can be found in the reference [16].

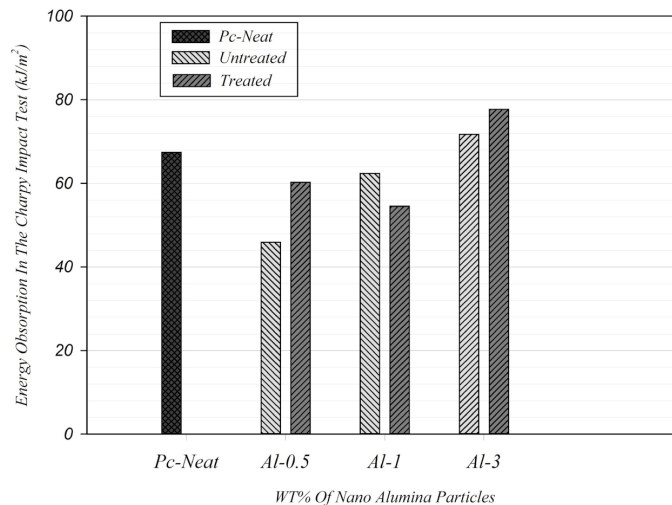
The effect of increasing alumina nano-contents in the nano-composites on their ballistic limit velocity has been illustrated in Fig. 10. Taking this figure and above explanation into consideration, it is obvious that all specimens contained treated or untreated alumina nanoparticles, and in all kinds of projectiles' hitting, the ballistic limit velocity increased as the weight percentage of alumina nano-fillers raised. However, in the specimens containing 0.5% and 1% (wt) of alumina nanoparticles, the ballistic limit velocity was lower than those for the neat polycarbonate. This had already been observed in the Charpy Impact Tests [16]. Here is a probable

Table 4. Jonas-Lambert equation and its coefficients for the best fit plot of all of the specimens under various projectiles hit

Specimens		$P$	Ballistic limit (m/s)	Coefficients of Lambert-Jonas equation		Lambert-Jonas equation
				$A$	$B$	
Pc-neat	Cylindrical projectile	2	126.31	0.7189	11470	$V_r^2 = 0.7189V_i^2 - 11470$
	Hemispherical projectile	2	125.88	0.6601	10460	$V_r^2 = 0.6601V_i^2 - 10460$
	Conical projectile	2	123.71	0.7625	11670	$V_r^2 = 0.7625V_i^2 - 11670$
Al-No-T-0.5	Cylindrical projectile	1.75	68.56	0.7554	1234	$V_r^{1.75} = 0.7554V_i^{1.75} - 1234$
	Hemispherical projectile	2.25	66.78	0.6746	8601	$V_r^{2.25} = 0.6746V_i^{2.25} - 8601$
	Conical projectile	2	60.28	0.6992	2541	$V_r^2 = 0.6992V_i^2 - 2541$
Al-No-T-1	Cylindrical projectile	1.75	71.02	0.7441	1293	$V_r^{1.75} = 0.7441V_i^{1.75} - 1293$
	Hemispherical projectile	1.75	69.84	0.7664	1293	$V_r^{1.75} = 0.7664V_i^{1.75} - 1293$
	Conical projectile	2	72.74	0.6788	2595	$V_r^2 = 0.6788V_i^2 - 2595$
Al-No-T-3	Cylindrical projectile	2	143.70	0.8576	17710	$V_r^2 = 0.8576V_i^2 - 17710$
	Hemispherical projectile	2	134.23	0.8469	15260	$V_r^2 = 0.8469V_i^2 - 15260$
	Conical projectile	2	129.85	0.8469	14280	$V_r^2 = 0.8469V_i^2 - 14280$
Al-T-0.5	Cylindrical projectile	2	116.71	0.8512	20630	$V_r^2 = 0.8512V_i^2 - 20630$
	Hemispherical projectile	2	109.22	0.7074	8439	$V_r^2 = 0.7074V_i^2 - 8439$
	Conical projectile	2	106.99	0.7078	8102	$V_r^2 = 0.7078V_i^2 - 8102$
Al-T-1	Cylindrical projectile	1.75	154.35	0.9571	6469	$V_r^{1.75} = 0.9571V_i^{1.75} - 6469$
	Hemispherical projectile	2	143.73	0.7561	15620	$V_r^2 = 0.7561V_i^2 - 15620$
	Conical projectile	2	133.76	0.7685	13750	$V_r^2 = 0.7685V_i^2 - 13750$
Al-T-3	Cylindrical projectile	1.75	156.14	0.7920	5535	$V_r^{1.75} = 0.7920V_i^{1.75} - 5535$
	Hemispherical projectile	2	155.54	0.7808	18890	$V_r^2 = 0.7808V_i^2 - 18890$
	Conical projectile	2	152.24	0.9100	5385	$V_r^2 = 0.9100V_i^2 - 5385$

Table 5. The effect of projectiles' nose geometry on the ballistic limit velocities of nano-composites

Specimen	Cylindrical	Hemispherical	Conical	Difference between hemispherical and cylindrical (%)	Difference between conical and cylindrical (%)
Pc-neat	126.31	125.88	123.71	-0.34	-2.06
AL-NO-T-0.5	68.39	66.78	60.28	-2.35	-11.85
AL-NO-T-1	71.02	69.84	72.74	-1.66	2.42
AL-NO-T-3	143.70	134.23	129.85	-6.59	-9.64
AL-T-0.5	116.71	109.22	106.99	-6.42	-8.33
AL-T-1	154.35	143.73	133.76	-6.88	-13.34
AL-T-3	156.14	155.54	152.24	-0.38	-2.50

Fig. 9. Energy absorption ( $\text{kJ/m}^2$ ) graph for nano-composites and the neat polycarbonate [16]

explanation: although the alumina nano-contents cause an increase in the failure elongation in nano-composites in comparison with the neat polycarbonate [16], these two kinds of specimens do not have enough nano-fillers to generate ample reaction forces, and prevent the produced cracks from meeting each other. Better put, they do not disperse in their matrix uniformly to the degree that they finally go up the plastic deformation or, in other words, increase their ductility. Of course, in the specimens with 1 wt% of treated alumina nano-contents and all kinds of specimens containing 3 wt% of nanoparticles, this problem was resolved, and their ballistic limit velocities were higher than those for the neat polycarbonate specimen under the hitting of different kinds of projectiles.

In Table 6, different percentages of the ballistic limit velocity for various nano-composite specimens hit by projectiles with different kinds of nose geometry have been compared with the neat polycarbonate specimen. It is outlined in the

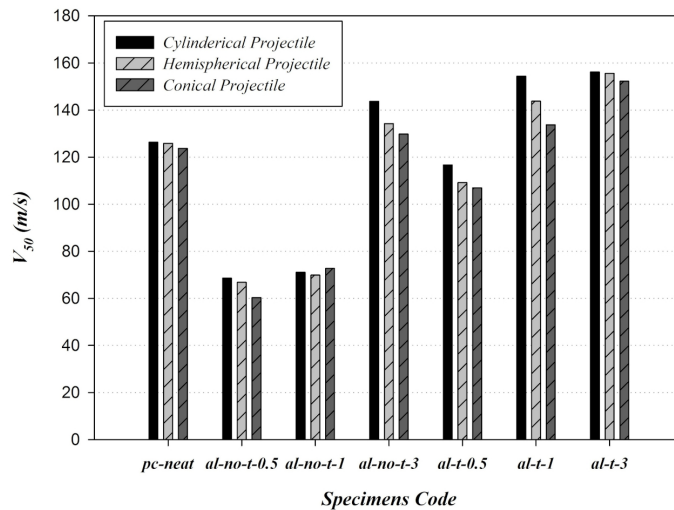


Fig. 10. The effect of increasing alumina nano contents in the nano-composites on their ballistic limit velocity

table that the ballistic limit velocity of nano-composites containing 1 and 3 weight percentage of treated alumina nanoparticles was at a higher rate compared to other specimens, in such a way that in the specimen Al-T-3, more than 23% of an increase in the ballistic limit velocity in hitting process of different kinds of projectiles was observed. Thus, it can be concluded that the specimen Al-T-3 had the best weight percentage and also the best dispersion and distribution of alumina nano-contents in the polycarbonate matrix in order to improve the ballistic limit velocity, compared to other specimens.

Table 6. The difference in percentage of the ballistic limit velocity of various nano-composite specimens hit by projectiles with different kinds of nose geometry in comparison to the neat polycarbonate specimen

Specimens	Difference percentage of ballistic limit velocity of specimens in comparison with the neat polycarbonate		
	Cylindrical	Spherical	Conical
Pc-Neat	–	–	–
Al-No-T-0.5	–45.86	–46.95	–51.27
Al-No-T-1	–43.73	–44.52	–41.20
Al-No-T-3	13.77	6.63	4.96
Al-T-0.5	–7.60	–13.23	–13.52
Al-T-1	22.20	14.18	8.12
Al-T-3	22.62	23.56	23.06

In Fig. 11, the impact of treatment process of the alumina nanoparticles on the ballistic limit velocity of the prepared nano-composites has been indicated.

As outlined in this figure, the treatment process caused the ballistic limit velocity of nano-composites to increase and improve. The coupling agent silane leads to stronger bonding between nanoparticles and polymer matrix [14, 16]. Therefore, it increases the level of energy absorption of nano-composites. It shows once more that the treating of alumina nanoparticles makes them have better dispersion and distribution in their polymer matrix, and the increase in the ballistic limit velocity is the result. The fact is that every accumulation in nano-composite plates caused the formation of cracks, due to the dynamic stress, to reach each other quickly. Also, it can be a good reason why the specimen Al-T-1 had a higher ballistic limit velocity in comparison with the neat polycarbonate, but the specimen Al-No-T-1 did not.

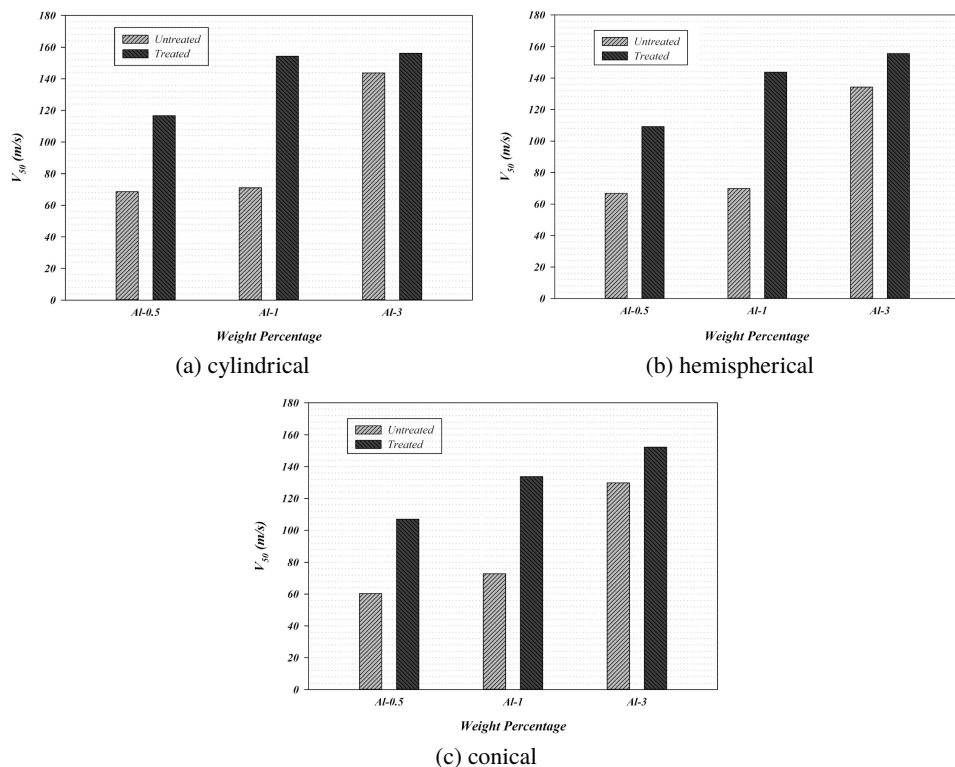


Fig. 11. The effect of treatment process of the alumina nanoparticles on the ballistic limit velocity of prepared nano-composites hit by various projectiles' nose geometry

## 5.2. Investigation on failure mechanism occurring in the specimens under the ballistic test

For the prevention of scattering the information and accessing the desirable results, in this part, the effect of changing the projectiles' nose geometry on the failure mechanisms, and also changes in these mechanisms resulting from the increase

of velocity, are investigated. This investigation was done only on the specimens that contained 3 %wt of alumina nanoparticles and got the largest quantity in the ballistic limit velocities among all other specimens. Besides, as it is mentioned in the introduction, generally, the failure mechanism of the polycarbonate plates is penetration, perforation, dishing, and petalling [6]. However, the combination of the above failure mechanisms has been observed during the tests. Indeed, owing to the inherent complexity of the composite materials, analyzing the failure mechanism is an ongoing research that might be vary from one case to others. Thus, it is decided to explain some plausible reasons about the mechanisms observed in the present work.

In this study, the common failure mechanism in all specimens was a plug separating from all target plates. A plug could be defined as a part of a target which is separated from it and has a diameter equal to the projectile's diameter. But the plugs in these targets had diameters bigger than the projectiles, where all different failure mechanisms happened. In other words, as it is mentioned earlier, the combination of failure mechanisms has been observed in the nano-composite targets. Changes in the failure mechanisms resulting from the increase in the velocity of conical projectiles in the plugs of specimen Al-T-3 has been illustrated in Fig. 12. It demonstrates that the failure mechanism was converted from dishing to petalling. Also, the perforations' diameter occurring in the plugs was reduced by increasing the conical projectiles' velocity. This has been illustrated in Table 7.



Fig. 12. Changing the failure mechanism resulted from velocity's rise of conical projectiles in the front and rear of the separated parts (plugs) of specimen Al-T-3 from dishing (no. 2) to petalling (no. 4 and 5)

Table 7. The reduction of perforations' diameter occurred in the separated parts (plugs) of specimen AI-T-3 by increasing the conical projectiles' velocity

Incident velocity (m/s)	Perforation's diameter (mm)
232.0	23.35
275.9	22.35
310.2	19.01
344.4	18.40
376.6	17.33

The previous phenomena were repeated once more in the hitting process of hemispherical projectiles, as presented in Fig. 13 and Table 8.

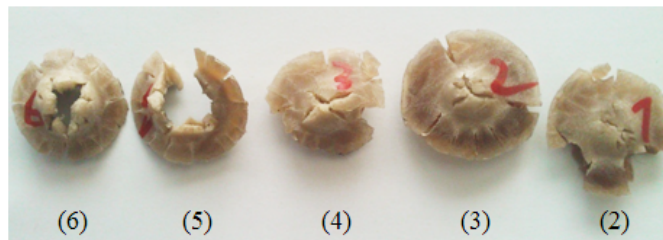


Fig. 13. Changing the failure mechanism resulted from velocity's rise of hemispherical projectiles in the separated parts (plugs) of specimen AI-T-3 from dishing to petalling (no. 2 to 5)

Table 8. The reduction of perforations' diameter occurring in the separated parts (plugs) of specimen AI-T-3 by increasing the hemispherical projectiles' velocity

Perforation's diameter (mm)	Incident velocity (m/s)
20.13	213.4
28.90	311.4
20.47	322.0
20.99	365.6
17.40	378.0

The reason for the combination of different failure mechanisms can be explained in this way: the initial stress wave caused a tensile stress in the material coming from bending in the place of target deformation. This stress was further greater than the dynamic yield stress of target material in quantity in the high strain rate, and hence led to the failure of material in that spot. By increasing the projectile's velocity, the perforation's depth (dish) made in the plug specimen elevated. But the stress waves did not have time to arrive at places in the target which are farther from the hitting point. Thus, while the perforation's depth in the separated part of the target (plug) increased, the perforation's diameter in the target plate decreased. Consequently, by increasing the projectile's velocity more and more,

the perforation's depth deepened more and more, until the stress outweighed the dynamic yield stress in the plug's material. Therefore, the dishing mechanism reformed to petalling. Naturally, the perforation's depth in the target plate (or plug's diameter) was reduced, as well.

Also, this mechanism happened in the cylindrical projectile's hit. Yet, the difference was in the low velocity of the cylindrical projectile, where the failure mechanism in the separated parts (plugs) was radial breaks, and in the higher impact velocity of projectile, one part of the material (called the local plug), with a diameter equal to the projectile's diameter, separated from the parts which had separated already from the target plate (with a bigger diameter called plug). This has been indicated for specimen Al-No-T-3 in Fig. 14.



Fig. 14. The local plugging mechanism occurring in the nano-composite targets Al-No-T-3 under the cylindrical projectiles' impact

The nano-composite specimens containing 3%wt of treated alumina nanoparticles, and hit by conical projectiles, were used in a specific manner in order to investigate the effect of weight proportion of nano-contents on the perforations' diameter produced in the nano-composite target plates. Table 9 outlines the reduction of perforations' diameter in these specimens.

Table 9. The reduction of perforations' diameter in the nano-composite targets produced by conical projectiles in the incident velocity of  $v_i = 344$  m/s with increasing in the weight percentage of nano-contents

Specimens	Pc-neat	Al-No-T-0.5	Al-No-T-1	Al-No-T-3	Al-T-0.5	Al-T-1	Al-T-3
Perforations' diameter (mm)	20.08	21.96	17.27	16.66	23.79	17.09	18.40

As it is observed in the table, as the weight percentage of nano-contents increased, the perforations' diameter decreased. The reason was the increase in the strength of nano-composites resulting from enhancing the proportion of nano fillers which resulted in further absorbing of energy that had already been discussed in the above sections [16], as shown in Fig. 5. For better apprehension, a criterion line has been drawn from the perforations' edge.



Fig. 15. The reduction of perforations' diameter produced in the nano-composite targets contained untreated nano particles by increasing the weight percentage of nano contents (from left to right of illustration; dimensions are in millimeter)

## 6. Conclusions

In this paper, the effect of alumina nano particles on the impact resistance of polymer composites was investigated. For this purpose, from among all polymers, a polycarbonate was chosen as a matrix of polymer nano-composite, owing to its special engineering properties. Then, by taking other papers and production conditions into account, nano fillers were mixed to the polycarbonate matrix in three weight percentages of 0.5%, 1% and 3%, using an extruder. Also, to make better dispersion and distribution of nano contents in the polymer matrix, some nano-composites containing alumina nanoparticles, which had already been treated by a coupling agent silane APTES were prepared. Finally, 130 specimens were produced for the ballistic tests via an injection molding process and hit by three different projectiles' noses (cylindrical, hemispherical and conical) in the approximate velocities' range of 80 m/s to 380 m/s. Generally, the results indicated that adding a certain amount of alumina nanoparticles could provide a higher ballistic resistance for the polycarbonate. However, many crucial factors should be considered during the manufacturing process in order to disperse and distribute the particles uniformly to obtain the desired outcomes. Moreover, treating the reinforcements could clearly improve the results. Also, considering the intricacy of mechanisms of failure in polymer composites, it was decided to find plausible answers to explain them; while further investigations need to take them into account. The most important conclusions from the empirical tests are:

1. The highest ballistic limit velocity was in the specimen Al-T-3, which increased the ballistic limit velocity by about 23% compared to a neat polycarbonate target.
2. The ballistic limit velocity of targets containing different %wt of nanoparticles increased by blunting the projectiles' nose geometry from conical to cylindrical.
3. It was highlighted that the treatment process of the alumina nanoparticles with the coupling agent silane APTES caused the prepared nano-composites to have higher ballistic limit velocity than the nano-composites containing untreated alumina nano particles in all %wt.

4. In all the test specimens, one part of the targets with the diameter greater than projectiles' diameter was separated from them, and that was where different failure mechanisms (according to the type of projectiles' nose geometry) occurred.
5. Ballistic tests indicated that in the conical and hemispherical projectiles' hitting, the failure mechanism was converted from dishing to the petalling, by raising the projectiles' velocity; whereas for the cylindrical projectiles, local plugging was in the failure mode.
6. The perforations' diameters produced in the target plates were reduced by increasing the proportion of particles, and also the projectile's velocity (with the same nose geometry).

## References

- [1] S. Fu, Y. Wang, and Y. Wang. Tension testing of polycarbonate at high strain rates. *Polymer Testing*, 28(7):724–729, 2009. doi: [10.1016/j.polymertesting.2009.06.002](https://doi.org/10.1016/j.polymertesting.2009.06.002).
- [2] Q.H. Shah and Y.A. Abkar. Effect of distance from the support on the penetration mechanism of clamped circular polycarbonate armor plates. *International Journal of Impact Engineering*, 35(11):1244–125, 2008. doi: [10.1016/j.ijimpeng.2007.07.012](https://doi.org/10.1016/j.ijimpeng.2007.07.012).
- [3] Q.H. Shah. Impact resistance of a rectangular polycarbonate armor plate subjected to single and multiple impacts. *International Journal of Impact Engineering*, 36(9):1128–113, 2009. doi: [10.1016/j.ijimpeng.2008.12.005](https://doi.org/10.1016/j.ijimpeng.2008.12.005).
- [4] M.R. Edwards and H. Waterfall. Mechanical and ballistic properties of polycarbonate apposite to riot shield applications. *Plastic Rubber Composites*, 37(1):1-6, 2008. doi: [10.1179/174328908X283177](https://doi.org/10.1179/174328908X283177).
- [5] I. Livingstone, M. Richards, and R. Clegg. Numerical and experimental investigation of ballistic performance of transparent armour systems. Lightweight Armour Systems Symposium Conference, UK, 10-12 November, 1999.
- [6] S.C. Wright, N.A. Fleck, and W.J. Stronge. Ballistic impact of polycarbonate—An experimental investigation. *International Journal of Impact Engineering*, 13(1):1-20, 1993. doi: [10.1016/0734-743X\(93\)90105-G](https://doi.org/10.1016/0734-743X(93)90105-G).
- [7] M. Rahman, M. Hosur, S. Zainuddin, U. Vaidya, A. Tauhid, A. Kumar, J. Trovillion, and S. Jeelani. Effects of amino-functionalized MWCNTs on ballistic impact performance of E-glass/epoxy composites using a spherical projectile. *International Journal of Impact Engineering*, 57:108–118, 2013. doi: [10.1016/j.ijimpeng.2013.01.011](https://doi.org/10.1016/j.ijimpeng.2013.01.011).
- [8] S.G. Kulkarni, X.L. Gao, S.E. Horner, J.Q. Zheng, and N.V. David. Ballistic helmets – Their design, materials, and performance against traumatic brain injury. *Composite Structures*, 101:313–331, 2013. doi: [10.1016/j.compstruct.2013.02.014](https://doi.org/10.1016/j.compstruct.2013.02.014).
- [9] W. Al-Lafi, J. Jin, and M. Song. Mechanical response of polycarbonate nanocomposites to high velocity impact. *European Polymer Journal*, 85:354-262, 2016. doi: [10.1016/j.eurpolymj.2016.10.048](https://doi.org/10.1016/j.eurpolymj.2016.10.048).
- [10] A. Kurzawa, D. Pyka, and K. Jamroziak. Analysis of ballistic resistance of composites with EN AW-7075 matrix reinforced with Al<sub>2</sub>O<sub>3</sub> particles. *Archive of Foundry Engineering*, 20(1):73–78, 2020. doi: [10.24425/afe.2020.131286](https://doi.org/10.24425/afe.2020.131286).
- [11] P.H.C. Camargo, K.G. Satyanarayana, and F. Wypych. Nanocomposite: synthesis, structure, properties and new application opportunities. *Materials Research*, 12(1):1-39, 2009. doi: [10.1590/S1516-14392009000100002](https://doi.org/10.1590/S1516-14392009000100002).

- [12] R. Jacob, A.P. Jacob, and D.E. Mainwaring. Mechanism of the dielectric enhancement in polymer–alumina nano-particle composites. *Journal of Molecular Structure*, 933(1-3):77–85, 2009. doi: [10.1016/j.molstruc.2007.05.041](https://doi.org/10.1016/j.molstruc.2007.05.041).
- [13] X. Zhang and L.C. Simon. In situ polymerization of hybrid polyethylene-alumina nanocomposites. *Macromolecular Materials and Engineering*, 290(6):573–583, 2005. doi: [10.1002/mame.200500075](https://doi.org/10.1002/mame.200500075).
- [14] S. Zhao, L.S. Schadleer, R. Duncan, H. Hillborg, and T. Auletta. Mechanisms leading to improved mechanical performance in nanoscale alumina filled epoxy. *Composites Science and Technology*, 68(14):2965–2975, 2008. doi: [10.1016/j.compscitech.2008.01.009](https://doi.org/10.1016/j.compscitech.2008.01.009).
- [15] S.C. Zunjarrao and R.P. Singh. Characterization of the fracture behavior of epoxy reinforced with nanometer and micrometer sized aluminum particles. *Composites Science and Technology*, 66(13):2296–2305, 2006. doi: [10.1016/j.compscitech.2005.12.001](https://doi.org/10.1016/j.compscitech.2005.12.001).
- [16] S. Amirchakmaghi, A. Alavi Nia, Gh. Azizpour, and H. Bamdadi. The effect of surface treatment of alumina nanoparticles with a silane coupling agent on the mechanical properties of polymer nanocomposites. *Mechanics of Composite Materials*, 51(3):347–358, 2015. doi: [10.1007/s11029-015-9506-7](https://doi.org/10.1007/s11029-015-9506-7).
- [17] E.A. Ferriter, A. McCulloh, and W. deRosset. Techniques used to estimate limit velocity in ballistic testing with small sample size. In *Proceedings of the 13th Annual U.S. Army Research Laboratory Conference*, pages 72–95, USA, 2005.
- [18] [www.plastics.bayer.com/Products/Makrolon/ProductList/201305212210/Makrolon-2807.aspx](http://www.plastics.bayer.com/Products/Makrolon/ProductList/201305212210/Makrolon-2807.aspx); Bayer MaterialScience AG., Polycarbonates Business Unit., (2013).
- [19] A. Chandra, L.S. Turng, P. Gopalan, R.M. Rowell, and S. Gong. Study of utilizing thin polymer surface coating on the nanoparticles for melt compounding of polycarbonate/alumina nanocomposites and their optical properties. *Composites Science and Technology*, 68(3-4):768–776, 2008. doi: [10.1016/j.compscitech.2007.08.027](https://doi.org/10.1016/j.compscitech.2007.08.027).
- [20] Z. Zatorski. Diagnostics of ballistic resistance of multi-layered shields. *Archive of Mechanical Engineering*, 54(3):205–218, 2007. doi: [10.24425/ame.2007.131555](https://doi.org/10.24425/ame.2007.131555).
- [21] H. Motulsky and A. Christopoulos. Fitting Models to Biological Data Using Linear and Non-linear Regression, a Particle Guide to Curve Fitting. GraphPad Software Inc., San Diego CA, 2003.